Theoretical & Applied Mechanics Letters 7 (2017) 164–168

Contents lists available at ScienceDirect

Theoretical & Applied Mechanics Letters

journal homepage: www.elsevier.com/locate/taml

Letter

Calculating buoy response for a wave energy converter—A comparison of two computational methods and experimental results

Linnea Sjökvist [a,b,*], Malin Göteman [a], Magnus Rahm [a], Rafael Waters [a], Olle Svensson [a], Erland Strömstedt [a], Mats Leijon [a]

[a] Division of Electricity, Department of Engineering Science, The Ångström Laboratory, Uppsala University, Box 534, 75121 Uppsala, Sweden
[b] Center for Natural Disaster Science (CNDS), Villavägen 16, SE-752 36 Uppsala, Sweden

HIGHLIGHTS

- Added mass, radiation damping and exciting force are calculated using a COMSOL model.
- The hydrodynamic parameters are compared to parameters from WAMIT.
- The equations of motion for a WEC are solved to find buoy movement and line force.
- Force and motion are compared to experimental offshore data, showing good agreement.

ARTICLE INFO

Article history:
Received 28 February 2017
Received in revised form 22 May 2017
Accepted 23 May 2017
Available online 1 July 2017
*This article belongs to the Fluid Mechanics.

Keywords:
Hydrodynamic simulation
Linear potential flow theory
Experiments
Wave energy
Lysekil research site

ABSTRACT

When designing a wave power plant, reliable and fast simulation tools are required. Computational fluid dynamics (CFD) software provides high accuracy but with a very high computational cost, and in operational, moderate sea states, linear potential flow theories may be sufficient to model the hydrodynamics. In this paper, a model is built in COMSOL Multiphysics to solve for the hydrodynamic parameters of a point-absorbing wave energy device. The results are compared with a linear model where the hydrodynamical parameters are computed using WAMIT, and to experimental results from the Lysekil research site. The agreement with experimental data is good for both numerical models.

In the Lysekil project, a point absorbing wave energy converter (WEC) technology is studied. The project is run by the Division of Electricity, Uppsala University, Sweden. A linear generator on the seabed is directly driven by a buoy floating on the water surface. The project started in 2002, and several prototypes have been deployed offshore at the Lysekil research site.

In the design process of any wave power concept, it is important to correctly model both average and peak loads on the WECs in order to build a WEC that can withstand the harsh environment offshore, and still keep the cost at an acceptable level. Extensive analytical work has been done on optimizing energy absorption by point-absorbing floating bodies restrained by linear power take-off system (PTO) and for monochrome waves during the 1970s [1–5]. If a linear PTO and regular waves with small amplitude are assumed, the hydrodynamic forces on the floating body can be decomposed into hydrodynamical parameters, and the WEC's behavior can be modeled numerically in the frequency domain [6,7]. Time-domain modeling based on the hydrodynamical parameters was developed in the 1980s [8]. In the Lysekil project, hydrodynamic modeling of the buoy movement in response to the incident waves has previously been performed using WAMIT [9,10], a commercial software in which it has been shown that verification to both large-scale and small-scale experiments shows acceptable agreement for wave climates that coincide with the normal working conditions [11]. WAMIT is a boundary integral equation method (BIEM) working in the frequency domain. It uses linear potential wave theory, which is a good enough approximation for simulations of small waves and linear loads. In the Lysekil project, that means wave climates for normal operating conditions, and a linear load on the generator. However, a grid-connected WEC might require a control system resulting in non-linear loads in the

* Corresponding author at: Division of Electricity, Department of Engineering Science, The Ångström Laboratory, Uppsala University, Box 534, 75121 Uppsala, Sweden.
E-mail address: linnea.sjokvist@angstrom.uu.se (L. Sjökvist).

http://dx.doi.org/10.1016/j.taml.2017.05.004

PTO, which would require hydrodynamic simulations in the time-domain [6].

To build a simulation model suited for the Lysekil research site in which non-linear effects can be accounted for, it is suggested to use the finite element method (FEM). In this paper, the commercial software COMSOL Multiphysics, using FEM, is used to compare simulated hydrodynamic parameters calculated in a COMSOL model with parameters calculated in WAMIT. The hydrodynamic parameters are used to calculate the buoy response for an incident wave. The equation of motion for the WEC is solved and the buoy position is modeled together with the expected force in the buoy line. The simulated values are compared with experimental data. The experimental work with the WEC used in this paper have been described earlier [12,13], while this paper focuses on the hydrodynamic simulations, to compare the BIEM solver WAMIT with the FEM solver COMSOL and to validate the models with experimental results. Linear theory is used in this paper.

The fluid is assumed to be inviscid and incompressible, and the flow is assumed to be irrotational. Laplace equation is defined and solved for in the water domain:

$$\nabla^2\phi = 0, \tag{1}$$

where the velocity potential ϕ is defined as the scalar potential of the velocity vector $\bar{\boldsymbol{v}}$, so that $\bar{\boldsymbol{v}} = \bar{\nabla}\phi$. In linear wave theory, the velocity potential can be described as a sum of the incident, the radiated, and the diffracted wave, ϕ_I, ϕ_R, and ϕ_D:

$$\phi = \phi_\mathrm{I} + \phi_\mathrm{R} + \phi_\mathrm{D}. \tag{2}$$

The total pressure field in a fluid is related to the velocity potential by the linearized Bernoulli equation [14]. The total pressure P is given by:

$$\begin{aligned} P(x, y, z, t) &= p(x, y, z, t) + p_s(z) \\ &= \rho\frac{\partial\phi(x, y, z, t)}{\partial t} - \rho g z, \end{aligned} \tag{3}$$

where p is the dynamic pressure and p_s describes the hydrostatic pressure and ρ is the density. If the pressure field is known, the force $\bar{F}$ on a submerged body can be derived from the velocity potential by integrating over the pressure on the wetted surface:

$$\bar{F} = \iint P \cdot \bar{n}\mathrm{d}S. \tag{4}$$

WAMIT is a radiation/diffraction 3D panel program for linear analysis of the interaction between surface gravity waves and offshore structures. The linearized boundary value problem is solved using Green's theorem by integrating the diffraction and radiation velocity potentials in closed surfaces. Excitation force, radiation damping and added mass are extracted from WAMIT for a rigid cylindrical buoy restricted to move in heave only. The buoy radius is 1.5 m and the draft is 0.4 m; the dimensions of the simulated buoy are identical to the buoy used in the experiments that are used for validation in this paper. The hydrodynamical parameters output from WAMIT is used as input in a linear MATLAB model described in Ref. [9] to compute the motion and line force of a WEC.

COMSOL Multiphysics is a commercial simulation software, capable of performing both stationary and time dependent multi-coupled physics problems. In this paper, COMSOL Multiphysics has been used to compute the hydrodynamical parameters, which have then been used as input in the same MATLAB model to compute the motion and line forces as for the WAMIT case. In COMSOL Multiphysics, a 3D model has been built, where the simulation domain consists of a cylindrical water domain where the Laplace equation is solved. The water domain has a radius R_d and a depth of 25 m. The buoy displacement has a radius of 1.5 m and a draft of 0.4 m. The model is solved for the frequency range from $\omega = 0.1$ rad/s to $\omega = 6$ rad/s, in steps of 0.1 rad/s. R_d is dependent on the frequency of the incoming wave, and is rebuilt for each ω. The mesh is also adapted to ω and is described below. In this paper, the time dependence in the velocity potential has been extracted [15], and stationary simulations have been performed:

$$\phi = Re(\phi_\mathrm{I} + \phi_\mathrm{D} + \phi_\mathrm{R})\mathrm{e}^{-\mathrm{i}\omega t}. \tag{5}$$

A deep water approximation has been made for the dispersion relation, $\omega^2 = gk$, where k is the wave number and g is the gravitational acceleration. On the water surface boundary, marked in Fig. 1(b), a free surface boundary condition is defined as:

$$\frac{\partial\phi}{\partial z} - k\phi = 0. \tag{6}$$

A radiating boundary condition is used to implement an incident wave in the model [16]. It is assumed that at an infinite distance r from the buoy, the diffracted and the radiated scalar velocity potential satisfies the condition:

$$\lim_{r\to\infty}\sqrt{kr}\left\{\frac{\partial(\phi_\mathrm{R} + \phi_\mathrm{D})}{\partial r} - \left[\mathrm{i}k - \frac{1}{2r}(\phi_\mathrm{R} + \phi_\mathrm{D})\right]\right\} = 0. \tag{7}$$

Equation (2) is substituted into Eq. (7) and is used as a boundary condition on the vertical surface far away from the buoy, the boundary marked in Fig. 1(c):

$$\left[\boldsymbol{n}\cdot\nabla\phi - \left(\mathrm{i}k - \frac{1}{2r}\right)\phi\right] - \left[\boldsymbol{n}\cdot\nabla\phi_\mathrm{I} - \left(\mathrm{i}k - \frac{1}{2r}\right)\phi_\mathrm{I}\right] = 0. \tag{8}$$

To evaluate the excitation force on a semi-submerged buoy, the scattered wave potential is evaluated by solving a diffracted boundary value problem. The buoy is held still in the water domain, and a known incident wave is implemented through the boundary condition described by Eq. (8). It should be noted that $\phi_\mathrm{R} = 0$ since the buoy is fixed in the water domain. The velocity potential of the incident wave is set to:

$$\phi_\mathrm{I} = \frac{Ag}{\omega}\mathrm{e}^{kz}\mathrm{e}^{-\mathrm{i}kx}, \tag{9}$$

where A is the amplitude of the incoming wave. In the model, the amplitude is set to 1 m. When COMSOL has solved for ϕ, the excitation force on the submerged buoy is derived from the velocity potential by integrating over the pressure on the bottom surface of the buoy, S:

$$F_\mathrm{e}(\omega) = Re\left(-\mathrm{i}\rho\omega\iint\phi\cdot\bar{n}\mathrm{d}S\right). \tag{10}$$

The excitation force has been calculated for heave.

The radiation force is calculated when the incident wave is set to zero, while the velocity potential from buoy movement is evaluated. To simulate buoy movement, a flow corresponding to a buoy velocity was set as a boundary condition on the bottom surface of the buoy:

$$\nabla\phi = 1. \tag{11}$$

The frequency dependent radiation force F_R is then:

$$F_\mathrm{R}(\omega) = \rho\omega^2\iint\phi_\mathrm{R}\cdot\bar{n}\mathrm{d}S = \omega^2 m_\mathrm{a} + \mathrm{i}\omega B(\omega), \tag{12}$$

where m_a is the added mass coefficient and $B(\omega)$ is the radiation damping coefficient. To find the radiation force in the time domain the convolution between the impulse response function and the velocity of the body can be performed.

The required resolution of the mesh is dependent on the simulated buoy size and the wavelength of the incident wave. A finer mesh is needed for the higher frequencies. A larger simulation

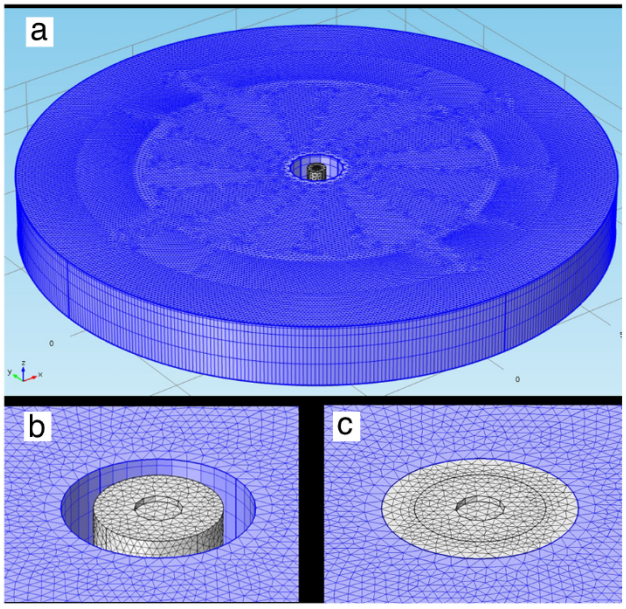

Fig. 1. (a) The simulation domain is split in three domains in order to build an adapted mesh. (b) In the vicinity of the buoy, the mesh is fine throughout the full depth. In the outer domain the mesh is coarser for larger depths. (c) A middle domain is used to connect the inner and the outer domain with a tetrahedral mesh.

domain is needed for the lower frequencies with longer wavelengths, since the radiating boundary condition of Eq. (8) must be placed at a large enough distance from the buoy to be valid. In Ref. [17], a fixed simulation domain with a fixed mesh was used. A compromise was needed between domain size and mesh refinement in order to make the model solvable, and irregularities that is likely aliasing errors can be seen in the solution for the higher frequencies. In this paper, both the simulation domain and the mesh resolution are dependent of the frequency, and are rebuilt for each frequency step. The water domain radius R_d is set to be equal to 6 wavelengths, implying that for low frequencies, R_d is large and the mesh resolution is coarser, while for higher frequencies, R_d is smaller and the mesh is finer. The simulation domain is split into three domains in order to build the adapted mesh. In Fig. 1(a), the three meshing domains for $\omega = 2.1$ rad/s can be seen, where only the inner and the outer domain is meshed in this figure. The middle domain, meshed in Fig. 1(c), is used to connect the mesh in the inner and outer domain with a tetrahedral mesh, and is required to avoid meshing problems. The outer domain is first meshed with a triangular mesh on the free surface boundary. The maximum element size is set to one tenth of a wavelength, and the minimum element size is set to one twelfth of a wavelength. The mesh is then swept down to create a 3D mesh. The distribution of elements in the depth is not uniform; the element size is smaller closer to the surface since the velocity potential is decreasing with the depth.

For the inner domain, a fine mesh is used for the whole depth. The maximum element size is set to one tenth of a wavelength, and the minimum element size is set to one twelfth of a wavelength.

The surface of the middle domain is meshed with a triangular mesh with a maximum element size of one tenth of a wavelength. A tetrahedral mesh is used to connect the inner and the outer domain.

One of the full scale WECs deployed at the Lysekil research site, Sweden, is described. The experimental data from the WEC was recorded during 30 min in March 2007.

The WEC studied in the simulations in this paper is shown in Fig. 2. It is described by the equations of motions in Eqs. (13) and

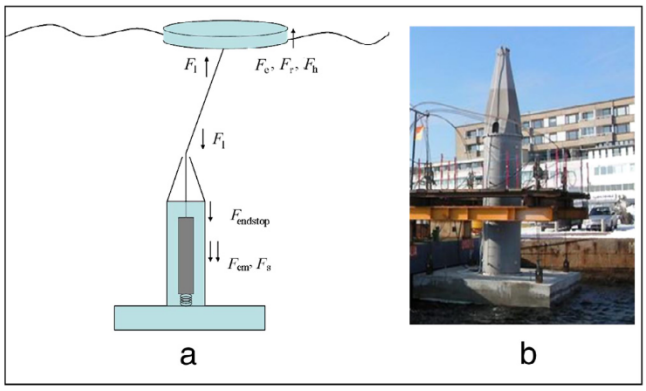

Fig. 2. Experimental setup. (a) Forces acting on the WEC. (b) The WEC before deployment.

(14), for the buoy and the translator respectively.

$$(m_a^{\infty} + m_b)\ddot{x}_b(t) = f_e * \eta(t) - K(t) * \dot{x}_b(t) + F_h + F_{line} - m_b g, \tag{13}$$

$$m_t\ddot{x}_t(t) = F_{line} - F_{em} - F_s + F_{endstop} - m_t g, \tag{14}$$

where $x_b(t)$ denotes the vertical buoy position and $x_t(t)$ the translator position. m_a^{∞}, m_b and m_t are the infinite added mass coefficient, the mass of the buoy and the mass of the translator. f_e is the radiation impulse response function for the excitation force, and η is the surface elevation, so that the excitation force is $F_e = f_e * \eta(t)$. $K(t) * \dot{x}_b(t)$ is the convolution between the radiation impulse response function and the velocity of the buoy, which gives the radiation force. F_h is the hydrostatic stiffness and F_{line} is the force in the buoy line. F_{em} is the electromagnetic force in the generator that transforms wave energy to electric energy. F_s is the retraction spring force in the early prototype design, which are exchanged to gravity in later prototype designs. $F_{endstop}$ is only active when the translator hits the endstop, which is when the wave amplitude exceeds the free piston length.

The WEC used in this experiment had a retraction spring with a spring coefficient $k_s = 6.2$ kN/m and a pretension of $k_{static} = 10$ kN so that:

$$F_s = -k_s x_t + k_{static}. \tag{15}$$

F_{em} is proportional to the translator velocity, and is described as:

$$F_{em} = -\gamma\dot{x}_t, \tag{16}$$

where γ is the damping coefficient which is dependent of the power that is delivered to the grid by the generator, and is possible to adjust with power electronics during operation. The damping coefficient is not defined if the velocity is zero.

This paper is analyzing data that was recorded during 30 min in March 2007, at the Lysekil research site. The sea state was recorded with a WaveriderTM wave measuring buoy placed 50 m from the WEC, which samples the wave elevation at 2.56 Hz. The significant wave height was 0.7 m during the time period, the time period was chosen so that the translator would not hit the endstop. The WEC was equipped with a cylindrical buoy with a radius of 1.5 m and a draft of 0.4 m in calm water. The buoy mass was 1000 kg and the translator mass was 1200 kg. In the buoy line, a force transducer (from HBM, U2B 200 kN) was placed and the line force, F_{line} was measured. An accelerometer (Analog Device ADXL202) was placed inside the buoy to measure relative position. The geometric data and the rating of this WEC have previously been

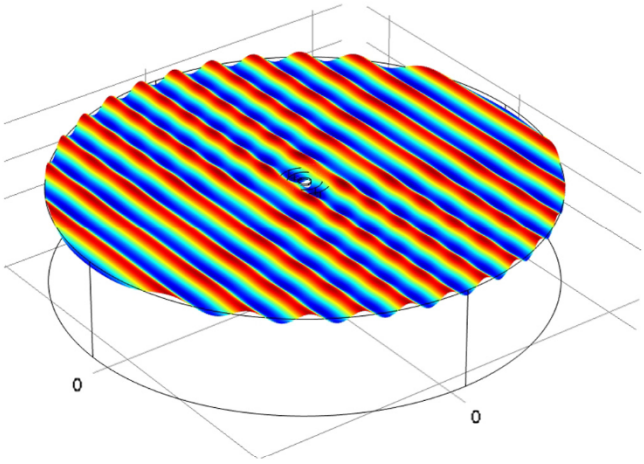

Fig. 3. The real part of ϕ, frequency of incident wave is $\omega = 2.5$ rad/s for this solution. The simulated water surface displacement is shown as a surface deformation.

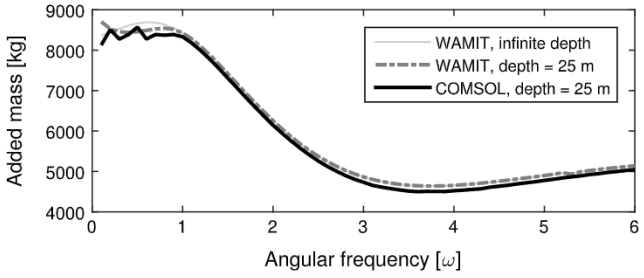

Fig. 4. Added mass in the frequency domain.

described in Ref. [18]. In this experiment a resistive load of 2.2 Ω was used. The damping coefficient for the WEC in this experiment was found experimentally by measuring the buoy velocity and position together with the line force and solving an average γ from Eq. (14). The translator was assumed to move with the buoy, and the measurement points where the velocity was zero were excluded from the calculation and the mean damping coefficient was found to be $\gamma \approx 27$ kN · s/m.

Hydrodynamical parameters were calculated in both COMSOL and WAMIT and compared. The equations of motion were solved to find the expected buoy movement and line force for a recorded sea state, which were compared to experimental results.

Figure 3 shows the solution to the diffraction problem when the COMSOL model is solved. The real part of the fluid potential ϕ is shown on the xz-plane where $z = 0$.

The excitation force, the added mass and the radiation damping simulated in COMSOL were compared to the same parameters simulated in WAMIT. In Fig. 4, the added mass from the COMSOL model is compared to the added mass from WAMIT. WAMIT was run both with an infinite depth and with a depth of 25 m, which is the same depth that was used in the COMSOL model and the depth at the Lysekil research site. The added mass simulated in COMSOL is slightly lower than the added mass simulated in WAMIT, but the frequency dependence is comparable. For low frequencies the COMSOL model shows an irregular behavior compared to the WAMIT model, and it is closer to the WAMIT solution for finite depth.

The radiation resistance is shown in Fig. 5. The behavior is comparable, but the FEM-values overestimate the radiation resistance slightly for frequencies $\omega > 2$ rad/s.

In Fig. 6, the absolute value of the excitation force is shown. The irregular behavior of the COMSOL simulation for high frequencies

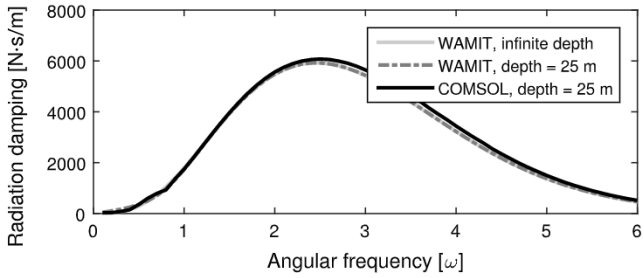

Fig. 5. Radiation resistance in the frequency domain.

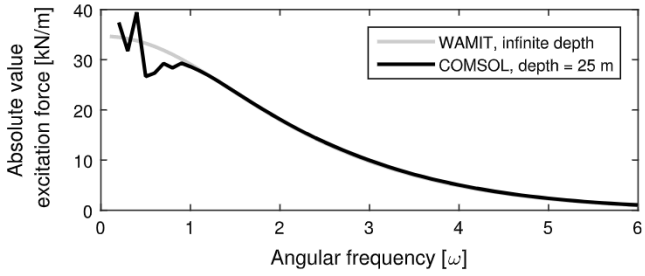

Fig. 6. Absolute value of excitation force.

that were seen in Ref. [17] is not present in this solution. The FEM simulation is comparable to the BIEM-simulation for frequencies higher than $\omega \approx 1$ rad/s. In Ref. [17], it was seen that the low frequency irregularities were reduced by using a larger simulation domain, and in this paper it can be seen that the irregularities were further reduced with the significantly larger simulation domain that was possible in this paper by combining the adapted domain size with the adapted mesh. The irregularities still present are assumed to derive from that the deep water approximation is not valid for the low frequencies. The authors have also used a deeper simulation domain, which resulted in further reduction of the irregularities, which supports this assumption. However, since the depth at the Lysekil research site is 25 m, this paper only presents FEM-simulation data using this depth. WAMIT was run assuming both an infinite depth and a depth of 25 m, but since the result was overlapping only the infinite depth result is shown in Fig. 6.

The buoy position and the force in the buoy line for the WEC have been measured, and a time series of 30 min recorded in March 2007 has been analyzed. By solving the equations of motion in the frequency domain, using the hydrodynamic parameters from the simulations, a response amplitude operator (RAO), was found. The convolution between the RAO and the recorded free surface gave the position of the buoy in response to wave motion. The method is described in Ref. [9]. In Fig. 7, the modeled vertical buoy position is shown. The water surface elevation recorded with the wave measuring buoy is used as input data. The simulations from WAMIT and COMSOL have the same shape, but the COMSOL signal is delayed in relation to the WAMIT signal. This can be derived from the fact that despite the excitation forces computed with WAMIT and COMSOL have almost identical absolute values of the excitation force, there is a phase difference between the two. The measured buoy position of the WEC for the same time period is also shown in Fig. 7. It should be noted that the measured and the simulated results are not expected to overlap since the wave measuring buoy and the WEC is placed 50 m apart. The simulated and the measured average buoy velocity over 30 min were calculated to allow for comparison between simulated and measured results, this is shown in Table 1. The measured water surface had an average vertical velocity of 0.43 m/s during those 30 min.

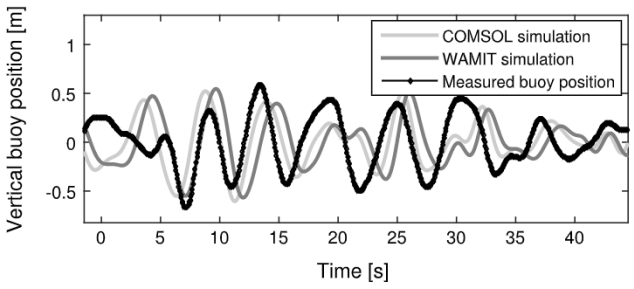

Fig. 7. Relative buoy position, modeled and measured values.

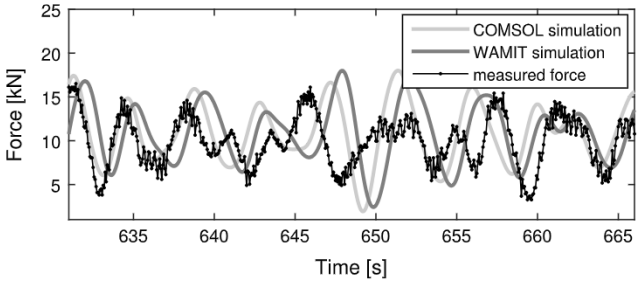

Fig. 8. Line force, calculated and measured values.

Table 1
Velocity and force results, average over 30 min.

	Vertical velocity	Line force
COMSOL	0.26 m/s	22 kN
WAMIT	0.26 m/s	22 kN
Experimental	0.25 m/s	20 kN

The measured line force on the WEC is shown in Fig. 8. The simulated buoy position from Fig. 7 was used in Eq. (13) to calculate the line force that the WEC would experience. To calculate the line force, it was assumed that the translator moved synchronized with the buoy. To be able to compare the measured and the simulated values, the mean values were taken over 30 min of measuring and are shown in Table 1. Even though the simulated and experimental results cannot be directly compared in phase, it can be seen that the amplitude and the frequency of the line force are comparable for the simulated and experimental results.

Overall, the simulated average buoy velocity and line force show good agreement with the experimental values. The wave climate at the Lysekil research site has been measured in Ref. [19], showing that the majority of the frequencies occurring at the test site will be between $\omega \approx 0.6$ and 3.5 rad/s. This means that it is likely that the irregularities in the excitation force and the added mass for low frequencies will not affect the simulated buoy response to real waves at this site significantly. When simulating forces for mechanical design it is the average and expected maximum forces for a wave climate that is interesting rather than precise buoy response to a single wave. Both models can be used for that.

The excitation force, the added mass and the radiation damping for a buoy have been simulated using two different computational approaches, and the results have been compared. The hydrodynamical parameters computed with the COMSOL model show good agreement with the ones computed using WAMIT. The hydromechanical parameters have been used to simulate buoy movement and velocity for a WEC at the Lysekil research site. Using the simulated buoy movement, the line force was calculated. The modeled buoy velocity and the calculated line force have been compared to experimental values from the Lysekil research site and show good agreement when the hydromechanical parameters from both the COMSOL model and from WAMIT were used. It is concluded that during normal operating conditions, where the translator does not hit the endstops, linear theory can be used to find both buoy movement and the force in the connection line to a reasonable accuracy using hydromechanical parameters from either the COMSOL model or WAMIT.

Acknowledgments

This research is supported by the Center for Natural Disaster Science (CNDS), the Swedish Research Council (VR, Grant Number 2015-04657), Lars Hiertas Foundation, and Bengt Ingeströms scholarship fund.

References

[1] S. Salter, Wave power, Nature 249 (1974) 720–724.
[2] K. Budal, J. Falnes, A resonant point absorber of ocean-wave power, Nature 256 (1975) 478–479.
[3] C. Mei, Power extraction from water waves, J. Ship Res. 20 (1976) 63–66.
[4] D. Evans, A theory for wave-power absorption by oscillating bodies, J. Fluid Mech. 77 (1976) 1–25.
[5] J. Falnes, A review of wave-energy extraction, Mar. Struct. 20 (2007) 185–201.
[6] A. Falcao, Wave energy utilization: a review of the technologies, Renew. Sustainable Energy Rev. 14 (2010) 899–918.
[7] D. Evans, Power from water waves, Ann. Rev. Fluid Mech. 13 (1981) 157–187.
[8] E. Jefferys, Device characterisation, Power from Sea Waves (1980) 413–438.
[9] M. Eriksson, J. Isberg, M. Leijon, Hydrodynamic modelling of a direct drive wave energy converter, Internat. J. Engrg. Sci. 43 (2005) 1377–1387.
[10] M. Eriksson, R. Waters, O. Svensson, J. Isberg, M. Leijon, Wave power absorption: Experiments in open sea and simulation, J. Appl. Phys. 102 (2007).
[11] G. Payne, J. Taylor, T. Bruce, P. Parkin, Assessment of boundary element method for modeling a free-floating sloped wave energy device. Part 2: Experimental validation, Ocean Eng. 35 (2008) 342–357.
[12] R. Waters, M. Stalberg, O. Danielsson, O. Svensson, S. Gustafsson, E. Strömstedt, M. Eriksson, M. Leijon, Experimental results from sea trials of an offshore wave energy system, Appl. Phys. Lett. 90 (2007).
[13] J. Engström, R. Waters, M. Stalberg, E. Strömstedt, M. Erikssona, J. Isberg, U. Henfridsson, K. Bergman, J. Asmussen, M. Lejon, Offshore experiments on a direct-driven wave energy converter, in: Proc. of the 7th Europeand Wave and Tidal Energy Conference, 2007.
[14] J.N. Newman, Marine Hydrodynamics, The Massachusetts Institute of Technology, 1977.
[15] S.A. Mavrakos, P. McIver, Comparison of methods for computing hydrodynamic characteristics of arrays of wave power devices, Appl. Ocean Res. 19 (1997) 283–291.
[16] R.T. Hudspeth, Waves and Wave Forces on Costal and Ocean Structures, World Scientific Publishing Co. Pte. Ltd., 2006.
[17] L. Sjökvist, J. Engström, S. Larsson, M. Rahm, J. Isberg, M. Leijon, Simulation of hydrodynamical forces on a buoy - a comparison between two computational approaches, in: Proceedings of the 1st Asian Wave and Tidal Energy Conference Series, South Korea, 27–30 November, 2012.
[18] M. Leijon, C. Bodström, O. Danielsson, S. Gustafsson, K. Haikonen, O. Langhamer, E. Strömstedt, M. Stalberg, J. Sundberg, O. Svensson, S. Tyrberg, R. Waters, Wave energy from the north sea: Experiences from the Lysekil research site, Surv. Geophys. 29 (2008) 221–240.
[19] R. Waters, J. Engström, J. Isberg, M. Leijon, Wave climate off the Swedish west coast, Renew. Energy 34 (2009) 1600–1606.